N. Dowson, M. Boult, P. Cowled, T. De Loryn, R. Fitridge

Development of an automated measure of iliac artery tortuosity that successfully predicts early graft-related complications associated with endovascular aneurysm repair

European Journal of Vascular and Endovascular Surgery, 2014; 48(2):153-160.

DOI: 10.1016/j.ejvs.2014.04.033

Development of an automated measure of iliac artery tortuosity that successfully predicts early graft-related complications associated with endovascular aneurysm repair

Nicholas Dowson[1], Margaret Boult[2], Prue Cowled[2], Tania De Loryn[2], Robert Fitridge[2]

[1]The Australian e-Health Research Centre, Computational Informatics, CSIRO, Royal Brisbane and Women's Hospital, Herston, QLD 4029, Australia

[2]Discipline of Surgery, The University of Adelaide, The Queen Elizabeth Hospital, 28 Woodville Road, Woodville South, SA 5011, Australia

Corresponding Author:

Professor Robert Fitridge

Discipline of Surgery, The University of Adelaide,

The Queen Elizabeth Hospital,

28 Woodville Road, Woodville South,

SA 5011, Australia

Phone: +61 8 8222 7711; Fax: +61 8 8222 6028; E-mail: evartrial@adelaide.edu.au

Category: Original Article

Short Title: Iliac tortuosity and EVAR complications

Word Count: 3994

What this paper adds

Iliac artery tortuosity has been linked to the likelihood of complications following endovascular aneurysm repair (EVAR). However, methodologies to calculate iliac tortuosity have remained subjective. It has also previously been unclear whether it is tortuosity at focal locations or for the vessel as a whole that is most relevant to deployment-related complications. This paper reports the development of a computerized CT imaging algorithm to accurately and reproducibly measure local curvature and calculate tortuosity indices. These measurements demonstrated that local tortuosity was significantly associated with early deployment-related complications after EVAR.

Abstract

Objectives: Iliac artery tortuosity has been linked to the likelihood of complications following endovascular aneurysm repair (EVAR). Measures of tortuosity can be established from CT images; however the reproducibility of existing scoring techniques has not been clearly established. It remains unclear whether it is tortuosity at focal locations or for the vessel as a whole that is most relevant to adverse events. Our two aims were firstly to develop an automated measure of iliac artery tortuosity to assist with surgical planning by providing an objective assessment of procedural difficulty and secondly, to correlate this measure with early post-operative outcomes.

Design and Methods: Unlike existing approaches, our measure of tortuosity considers spatial scale, which incorporates the effects of local anatomy. A computerized imaging algorithm was used to segment vasculature and establish a medial line and vascular boundary from contrast enhanced CT scans of 150 patients undergoing EVAR. Two tortuosity measures were examined: curvature and vessel to straight-line length (L_1/L_2-ratio). For a given spatial scale, the maximum tortuosity was computed on both iliac arteries and the artery with the lower maximum was selected for analysis. Correlation of tortuosity with early (<30 day) and longer-term graft-related complications was assessed.

Results: Maximal tortuosity at a 10mm scale was a significant predictor of early (<30 day) complications ($p=0.016$ for curvature and $p=0.006$ for L_1/L_2-ratio), but not of long-term complications. Aneurysmal diameter was independent of tortuosity (Pearson's r-value = -0.006).

Conclusion: The results demonstrate that, at a local scale, tortuosity measures are correlated with early outcomes. The spatial scale at which tortuosity is measured is

important. The optimal scale of 10mm implies that adverse events could be linked to a focal anatomical location.

Keywords:

Abdominal Aortic Aneurysm

Endovascular Procedures

Tomography, Computed, Scanners

Arterial Tortuosity

Analysis, Computer-Assisted Image

Image Interpretation, Computer Assisted

Introduction

Endovascular repair of abdominal aortic aneurysms (EVAR) is currently the preferred technique for individuals with suitable anatomy. A significant proportion of cases in which this technique is attempted develop graft-related complications[(1)]. Iliac artery tortuosity is a potent cause of these complications but has proven difficult to objectively measure with available techniques.

In previous work we showed that other anatomical factors (neck diameter, length and angulation) are strongly associated with mortality and morbidity after EVAR[(1)]. Not many studies have linked outcomes with iliac artery tortuosity, despite the difficulty of deploying a stent graft through a highly tortuous vessel. This may be due to tortuosity being evaluated subjectively. Boyle[(2)] noted that despite the "*potential influence that access vessel angulation can have on outcome, there is not a good, reliable, and repeatable measure of iliac angulation".*

In their reporting standards for EVAR, Chaikof[(3)] introduced an iliac artery tortuosity index L_1/L_2, where L_1 is the distance along the central lumen line between the common femoral artery and the aortic bifurcation and L_2 is the straight line distance between these points. They proposed this measure be included with iliac calcification and diameter for stratifying risk of access failure, but did not validate this with data.

A systematic review[(4)] examining protocols for determining 3-D aneurysm morphology using CT angiography highlighted a lack of information on intra- and inter-observer variability in measuring iliac tortuosity. Elsewhere, the same authors[(5)] reported good inter-observer

reproducibility, but did not link morphology to patient outcomes. They noted, "*automated methods are likely to be more suitable for certain measurements*". In a later study, Karthikesalingam[6] reported that iliac artery tortuosity was significantly associated with aortic complications after EVAR in univariate, but not multivariate analysis. Wyss[7] reported that iliac tortuosity (L_1/L_2) was associated with higher rates of graft-related complications after EVAR.

Several measures of tortuosity based on curvature are reported in the literature[8]. Wolf [9] described three measures of tortuosity that showed agreement between observer and computer measures, (albeit lower than inter-observer agreement): tortuosity index, which counts the number of segments with curvatures of less than $0.3cm^{-1}$, L_1/L_2-ratio over the entire iliac artery, and cumulative angulation, which sums the angles of all vessel bends from 2D projections of the 3D data. Wolf[9] also found significant associations between tortuosity indices and indicators of EVAR complexity (fluoroscopy time, amount of contrast, extender modules or vascular reconstruction). O'Flynn[10] also suggested including torsion when assessing vessel tortuosity. All of these measures integrate, and hence average, values over the entire artery. However, it is likely to be the most tortuous *local* regions from which procedural challenges arise. Iliac arteries where tortuosity is acute but localised, can report a low average tortuosity, but make for a technically challenging EVAR.

In this study an automated algorithm was used to extract the medial lines of the iliac arteries from contrast-enhanced CT images. The algorithm requires three seed (or marker) points to be manually placed in the centres of the superior aortic neck and mid common femoral arteries; no other input is required and minimal operator training is needed. From

the medial line accurate measurements of tortuosity were obtained and used to examine whether graft-related adverse events are a product of tortuosity at focal points, the "*focal source of problems*" hypothesis, or cumulatively for the vessel as a whole, the "*cumulative difficulty*" hypothesis.

Materials and Methods

Patient dataset

Prospective data and contrast-enhanced preoperative CT scans (n=150) were collected from patients in Australia undergoing elective EVAR between 2009 and 2012. Ethics approval was obtained from all institutions. Clinical data were collected pre-surgery, perioperative, 30 days post-surgery (or at discharge), and at 6, 12, 24 and 36 months. Mortality information came from the Australian Institute of Health and Welfare, National Death Index.

Measures of tortuosity were evaluated against early, (within 30 days) (defined in Table 1a) and late, (up to three years) (Table 1b) graft-related complications. Tortuosity was evaluated using a method specifically designed for purpose, that we have called *Tortuosity in Aorto-Iliac Pathology Nomogram* (TAIPAN), (a vessel delineation method[11],[12]).

Vascular Segmentation

The segmentation algorithm, TAIPAN, is described schematically in Figure 1. The method is automatic, apart from requiring three user-supplied seed points to be manually placed in the centres of the superior aortic neck and anterior femoral arteries. In steps 1 and 2, an intensity model is used to classify regions as "enhancing vasculature" or "other tissue".

Regions unconnected to the seed points are removed. In step 3, a customised path finding algorithm[13] is used to obtain an initial estimate of the medial vessel line between the three seed points. In step 4, a refined intensity model is created and, along with standard image morphology methods[14], is used to locate the lumen wall on each axial slice. The distance to the lumen wall within vessels is calculated in step 5, and utilising a second path-finding process, is used to refine the position of the medial line in step 6. Combining the boundary and medial lines gives the results shown in step 7. Steps 2-7 are all automatic; the sole user input is the 3 seed points at the start of the process.

Tortuosity Metrics

The path, ***p***, followed by the medial vessel line is an ordered set of discrete points in 3D space. The distance travelled along the medial line is defined by the scalar, *u*, where for a given artery, u=0 defines the inferior-most point in the femoral artery, with *u* increasing in the direction of the aorta. Hence the path taken by the medial vessel line can be thought of as a function ***p(u)***.

Defining the vessel medial line allows tortuosity to be quantified. Multiple measures of tortuosity exist, many of which are based on the mathematical measure of curvature, κ:

$$\kappa(u) = \left|\frac{d\boldsymbol{p}(u)}{du} \times \frac{d^2\boldsymbol{p}(u)}{du^2}\right| \left|\frac{d\boldsymbol{p}(u)}{du}\right|^{-3}, \qquad (1)$$

Since ***p*** is discrete, the derivatives of ***p*** with respect to *u* are computed using numerical differences, i.e. $\frac{d\boldsymbol{p}(u)}{du}$ is approximated by $\frac{p(u+\Delta u) - p(u)}{\Delta u}$. A choice can be made about the scale, Δu, over which the numerical differences are taken. The choice of scale is important as it means only anatomy at the scale of Δu is considered while anatomy outside

of this scale is ignored. This helps discern the scale most relevant to EVAR, reducing the effect of averaging over the entire vessel. Storing measures as functions of *u* allows the maximum local tortuosity to be computed.

To cover the full range of relevant anatomical structures that are visible in CT images, Δu varies on a logarithmic scale from 1mm to 100mm. At larger scales the maximum operation becomes similar to the mean, because the scale encompasses almost the entire artery and the measures vary only slightly with *u*.

Two iliac tortuosity values were obtained for each patient (left and right). Since the access vessel used for the main EVAR stent body was not generally recorded, access through the least tortuous artery was assumed. Hence the maximum tortuosity within the least tortuous vessel was reported (min-max tortuosity).

For the full range of scales (1-100mm), two tortuosity measures were examined: curvature:

$$\min_{\text{left ,right}} \max_{\text{u}} \kappa(u, \Delta u), \quad (2)$$

and L_1/L_2-ratio

$$\min_{\text{left ,right}} \max_{\text{u}} \frac{\int_{u_0-\Delta u/2}^{u_0+\Delta u/2} |\boldsymbol{p}(u)| du}{\Delta u}, \quad (3)$$

where the numerator is the medial line distance and Δu is the straight-line distance.

Selecting the optimal scale and testing for significance

To select the optimal scale, a Receiver Operating Characteristic (ROC) was computed for the measures in (2) and (3) at each scale, considering the sensitivity and specificity when predicting early and late problems.

ROC analysis considers the ranking of a given measure, but ignores the magnitude, so it doesn't consider whether samples with or without problems can be distinguished in the presence of measurement noise. Hence a Student's t-test was performed at the optimal scale to compare "early problems" and "no early problems" and similarly for late problems. The Student's t-test was included because it is possible to obtain a high Area under the Curve (AuC) and a low significance (high p-value). In this case, the measure would be sensitive to measurement error and not useful in practice. Conversely, distant outliers in each class could result in low AuC and high significance, also indicating a measure to be of low utility. Hence, to be acceptable a measure should have high AuC (predictive) and have significance (tolerant of measurement noise).

Pearson's correlation coefficient was used to examine whether a relationship existed between curvature and L_1/L_2-ratio or aneurysm diameter. Values close to zero indicate low correlation and *vice-versa* for values close to -1 or 1.

Results

There were 150 patients in this study, of whom 36 experienced early graft-related problems and 31 had late graft-related problems. Details of the problems for each patient are provided in the supplementary table. Of the 36 patients with early problems, 12 also had late graft-related problems.

Using the TAIPAN algorithm, the vessel tortuosities were measured for each CT image. Mean time to process each image was 22 seconds. The maximum tortuosity of the least

tortuous vessel was used to assess the predictive ability of curvature and the L_1/L_2-ratio for spatial scales from 1–100mm. Typical examples of low and high maximum tortuosities at a scale of 10mm, along with corresponding L1/L2-ratios are illustrated in Figure 2. The relatively languid undulations of the low tortuosity example can be contrasted against the sudden change in direction in the high tortuosity example.

The relationship between early graft-related problems and tortuosity is shown in Figure 3. Figure 3a shows one ROC curve per scale, plotted to assess whether curvature can discriminate between patients with and without early graft-related problems. The plot shows the 10mm scale is the optimum predictor of early problems (AuC 0.665). Figure 3c demonstrates the same for the L_1/L_2-ratio, with the 10mm scale also having the best AuC (0.651). In both Figures 3a and 3c, performance drops off rapidly as the scale increases, with no better than random performance at the maximum scale of 100mm (AuC 0.507 for curvature and 0.485 for L_1/L_2-ratio). The 100mm scale approximates taking a global (whole vessel) average. For both measures, the effect of reducing scale to 5mm or 2mm decreases performance only slightly, but a large drop in performance occurs for the 1mm scale.

We also measured the predictive performance of 10mm-scale tortuosity measures on early graft-related problems. Figures 3b & 3d show significant separation of classes for both curvature and L_1/L_2-ratio measures when fitting the Students t-test to samples with and without early graft-related problems. This separation allows the null hypothesis (tortuosity does not predict early problems) to be rejected with significance for curvature ($p=0.016$) and for L_1/L_2-ratio ($p=0.006$).

Figure 4 presents the ROC analysis of curvature (Figure 4a) and L_1/L_2-ratio (Figure 4b) for late problems. Neither measure was predictive, with no better than random performance at any scale.

Figure 5 shows that maximum aneurysm size has a limited correlation with early stent-related problems in this study. The AuC is 0.593 (Figure 5a) and the Student's t-test gave a p value of 0.0.051 (Figure 5b).

Most likely, curvature and L_1/L_2-ratio measure the same thing as indicated by their high correspondence in Figure 6a (Pearson's R-Value = 0.8832). To test whether aneurysm diameter and tortuosity are correlated, a Pearson's correlation coefficient was computed for these two variables at the optimal scale of 10mm (Figure 6b). The r-value for the two variables is almost zero indicating that the variables are probably independent.

Discussion

In this study we have developed an automated technique which measures iliac artery tortuosity. We demonstrate that a scale of 10mm is best for predicting the likely success of EVAR. We therefore assert that the "*focal source of problems*" hypothesis is true. In particular we assert that it is the most challenging (tortuous) region of the anatomy that is responsible for procedural difficulties. This probably relates to the relative size of the stent (width and length) and the anatomy through which it passes. If scale were not relevant then a wide range of scales would have similar predictive abilities with no drop-off in performance. Graft-related problems arising within 30 days were used as a proxy measure for procedural difficulty, however the rules for this assessment are well defined (Table 1).

Whether proximal or distal site of type-1 endoleaks influenced the result is unknown as this information was not collected.

Conversely, we have shown "*cumulative difficulty*" hypothesis to be false. It would only be true if tortuosity over a large range of scales predicted early stent-related problems. Testing showed the opposite occurred with a rapid drop in predictive performance as scale increased beyond 10mm, most likely because averaging measures of tortuosity over long segments of vessel returns low tortuosity values for vessels with a single acutely-angulated region. The "*focal source of problems*" hypothesis overcomes the adulterating effects of averaging by using spatial scale within tortuosity measures and hence is able to show the maximum tortuosity along the entire artery.

To be useful, the magnitude of tortuosity must distinguish between cases with and without early graft-related problems. Using Student's t-test, we show a clear and significant class separation for both curvature and L_1/L_2-ratio. That the results generalize across these two measures, with very similar ROCs, indicates that the relevance of scale is not an artifact of a particular measure. In addition, both measures identified a scale of 10mm as being optimal.

Interestingly, tortuosity was not linked to late graft-related problems. This is likely to be the case because a number of causes apart from tortuosity are likely to contribute to the development of late complications following EVAR.

The clinical implication of local tortuosity being predictive of early problems, is that tortuosity should be reported at all points in the vessel, rather than giving a single value for

the vessel as a whole. Such results should be reported in a form allowing the clinician to identify problematic regions at a glance, but also to explore and query the data at will. Hence the algorithm will need to be attached to existing DICOM image analysis software that is widely used by vascular surgeons and radiologists, for example, OsiriX (Pixmeo, Geneva, Switzerland).

Maximum aneurysm diameter is known to be a good predictor of survival[1] so we assessed whether it was indicative of early graft-related problems, and, if so, whether high tortuosity was simply a manifestation of the same phenomenon underlying dilated aneurysms. In fact, aneurysm diameter had a weak correlation with early problems, and no correlation with tortuosity, implying that the two variables are independent. Enlarged aneurysms and tortuosity are most likely indicative of different aspects of a complex biological process.

Our ability to assess the "*focal source of problems*" hypothesis depended on an automated method of delineating and extracting the required blood vessels from the contrast enhanced CT images. The TAIPAN algorithm was based on various historical approaches[15]. Some of the earliest successful arterial segmentation studies used multi-scale image filters to define a function of 'vesselness' as proposed by Frangi[16]. Where particular vessels require identification and selection, shortest path algorithms,[13],[17],[18] can be tailored for particular vessel extraction applications,[11],[12]. Despite the number of algorithms, some with freely available source code[19],[20],[21], few fully automatic methods are incorporated into commercial software, although semi-automatic approaches are available[22].

Future directions of this work will involve developing automated measures of calcification, given its likely contribution to the successful deployment of an EVAR graft and to postoperative problems. Given the success of the "*single-point of problems*" hypothesis, future work will assess the combined effect of focal tortuosity, calcification and vessel width.

Acknowledgements

Gillian Jagger
All contributing surgeons

Funding for this project was obtained from the National Health and Medical Research Council of Australia.

Conflicts of Interest

None

References

1. Barnes M, Boult M, Maddern G, Fitridge R. A model to predict outcomes for endovascular aneurysm repair using preoperative variables. Eur J Vasc Endovasc Surg. 2008;35(5):571-9.

2. Boyle JR, Thompson MM, Vallabhaneni SR, Bell RE, Brennan JA, Browne TF, et al. Pragmatic minimum reporting standards for endovascular abdominal aortic aneurysm repair. J Endovasc Ther. 2011 Jun;18(3):263-71.

3. Chaikof EL, Blankensteijn JD, Harris PL, White GH, Zarins CK, Bernhard VM, et al. Reporting standards for endovascular aortic aneurysm repair. J Vasc Surg. 2002;35(5):1048-60.

4. Ghatwary TM, Patterson BO, Karthikesalingam A, Hinchliffe RJ, Loftus IM, Morgan R, et al. A systematic review of protocols for the three-dimensional morphologic assessment of abdominal aortic aneurysms using computed tomographic angiography. Cardiovasc Intervent Radiol. 2013;36(1):14-24.

5. Ghatwary T, Karthikesalingam A, Patterson B, Hinchliffe R, Morgan R, Loftus I, et al. St George's Vascular Institute Protocol: an accurate and reproducible methodology to enable comprehensive characterization of infrarenal abdominal aortic aneurysm morphology in clinical and research applications. J Endovasc Ther. 2012;19(3):400-14.

6. Karthikesalingam A, Holt PJ, Vidal-Diez A, Choke EC, Patterson BO, Thompson LJ, et al. Predicting aortic complications after endovascular aneurysm repair. Br J Surg. 2013;100(10):1302-11.

7. Wyss TR, Dick F, Brown LC, Greenhalgh RM. The influence of thrombus, calcification, angulation, and tortuosity of attachment sites on the time to the first graft-related complication after endovascular aneurysm repair. J Vasc Surg. 2011;54(4):965-71.

8. Wesarg S, Khan MF, Firle EA. Localizing Calcifications in Cardiac CT Data Sets Using a New Vessel Segmentation Approach. J Digit Imaging. 2006;19(3):249-57.

9. Wolf YG, Tillich M, Lee WA, Rubin GD, Fogarty TJ, Zarins CK. Impact of aortoiliac tortuosity on endovascular repair of abdominal aortic aneurysms: evaluation of 3D computer-based assessment. J Vasc Surg. 2001;34(4):594-9.

10. O'Flynn PM, O'Sullivan G, Pandit AS. Methods for Three-Dimensional Geometric Characterization of the Arterial Vasculature. Ann Biomed Eng. 2007;35(8):1368-81.

11. Wink O, Niessen WJ, Viergever MA. Fast delineation and visualization of vessels in 3-D angiographic images. IEEE Transactions on Medical Imaging. 2000;19(4):337-46.

12. Liao W, Rohr K, Wörz S. Globally Optimal Curvature-Regularized Fast Marching for Vessel Segmentation. In: Mori K, Sakuma I, Sato Y, Barillot C, Navab N, editors. Medical Image Computing and Computer-Assisted Intervention. Lecture Notes in Computer Science: Springer Berlin Heidelberg; 2013. p550-7.

13. Dijkstra EW. A note on two problems in connexion with graphs. Numerische Mathematik. 1959;1(1):269-71.

14. Petrou M, Petrou C. Image Processing: The Fundamentals. 2nd Edition ed. Hoboken, New Jersey, USA: John Wiley and Sons, Ltd.; 2010.

15. Lesage D, Angelini ED, Bloch I, Funka-Lea G. A review of 3D vessel lumen segmentation techniques: Models, features and extraction schemes. Medical Image Analysis. 2009;13(6):819-45.

16. Frangi AF, Niessen WJ, Vincken KL, Viergever MA. Multiscale vessel enhancement filtering. In: Wells WM, Colchester A, Delp S, editors. Medical Image Computing and Computer-Assisted Interventation. Lecture Notes in Computer Science: Springer Berlin Heidelberg; 1998. p130-7.

17. Johnson DB. A Note on Dijkstra's Shortest Path Algorithm. J ACM. 1973;20(3):385-8.

18. Lorensen WE, Cline HE. Marching cubes: A high resolution 3D surface construction algorithm. SIGGRAPH Comput Graph. 1987;21(4):163-9.

19. Sato Y, Nakajima S, Shiraga N, Atsumi H, Yoshida S, Koller T, et al. Three-dimensional multi-scale line filter for segmentation and visualization of curvilinear structures in medical images. Medical Image Analysis. 1998;2(2):143-68.

20. Antiga L, Steinman DA. Robust and objective decomposition and mapping of bifurcating vessels. IEEE Transact Medical Imaging. 2004;23(6):704-13.

21. Piccinelli M, Veneziani A, Steinman DA, Remuzzi A, Antiga L. A Framework for Geometric Analysis of Vascular Structures: Application to Cerebral Aneurysms. IEEE Transact Medical Imaging. 2009;28(8):1141-55.

22. Krishnamoorthy P, Brejl M, van Ooijen PMA. System for Segmentation and Selective Visualization of the Coronary Artery Tree for Evaluation of Stenosis, Soft Plaque and Calcification in Cardiac CTA. Imaging Decisions MRI. 2004;8(2):25-30.

Table 1a: Definitions for early stent-related problems

Complications at time of procedure & prior to discharge	**Inclusions**: Operative complications, vessel complications, misplaced deployment, failed deployment, distal embolisation, failed access, twist/kink/obstruction, type-1 endoleak, type-3 endoleak, migration, thrombosis, stenosis, graft-thrombosis, broken/damaged wires. **Exclusions:** Type 2, & 4 endoleak
Unplanned procedures at the time of the operation or prior to discharge for aneurysm or graft	**Inclusions**: Unplanned procedures pertaining to aneurysm or graft **Exclusions**: Open groin repair, femoral cut down
Death	**Inclusions:** Death ≤30 days

Table 1b: Definitions for late (>30 days) stent-related problems

Late post-operative problems	**Inclusions:** Type-1 or type-3 endoleak, kinking, migration, graft thrombosis, broken/damaged wires, stenosis **Exclusions:** Type 2 & 4 endoleak, femoral bifurcation scarring / bleeding
Reoperation for aneurysm	**Inclusions:** Aneurysm or graft-related procedure **Exclusions**: Repairs for type 2 endoleaks (embolisation)
Death	**Inclusions:** Aneurysm-related (rupture) **Exclusions**: Death from other causes

Figure Legends

Figure 1:

Schematic diagram of vessel segmentation algorithm

Figure 2:

Examples of low and high maximum tortuosities at a scale of 10mm are shown, along with corresponding L1/L2-ratios.

Figure 3:

Ability to predict early (≤30 day) problems using the least tortuous artery 1mm to 100mm scales (NEP: No early graft-related problems; EP: early graft-related problems)

(a) ROC analysis of curvature

(b) Ability of curvature at 10mm scale to predict early problems

(c) ROC analysis of L_1/L_2-ratio

(d) Ability of L_1/L_2-ratio at 10mm scale to predict early problems

Figure 4:

Ability to predict late (up to 3years) problems using the least tortuous artery at 1mm to 100mm scales

(a) ROC analysis of curvature

(b) ROC analysis of L_1/L_2-ratio

Figure 5:

Ability of maximum aneurysm diameter to predict early (≤30d) problems

(a) ROC analysis

(b) Linear Regression Analysis

Figure 6:

(a) Pearson's correlation coefficient between maximum curvature and L_1/L_2-ratio

(b) Pearson's correlation coefficient between maximum curvature and maximum aneurysm diameter

Figure 1
Click here to download Figure(s): EJVES9226R rev1 Revised Figure 1.pdf

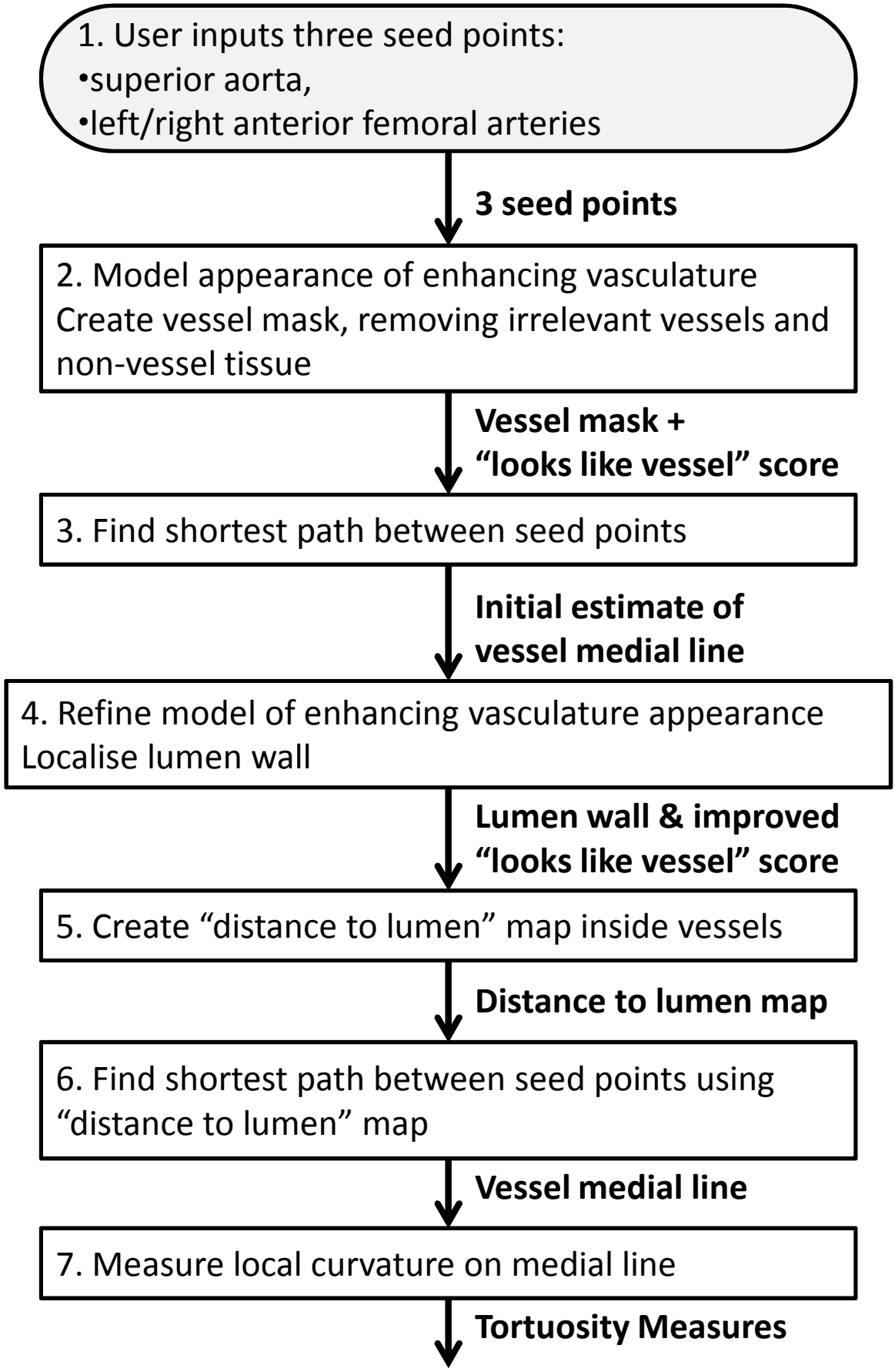

Figure(s)

Example of *low* tortuosity medial line (using $\frac{L_1}{L_2}$-ratio)

Click here to download Figure(s): EJVES9226R rev2 NEW Figure 2.pdf

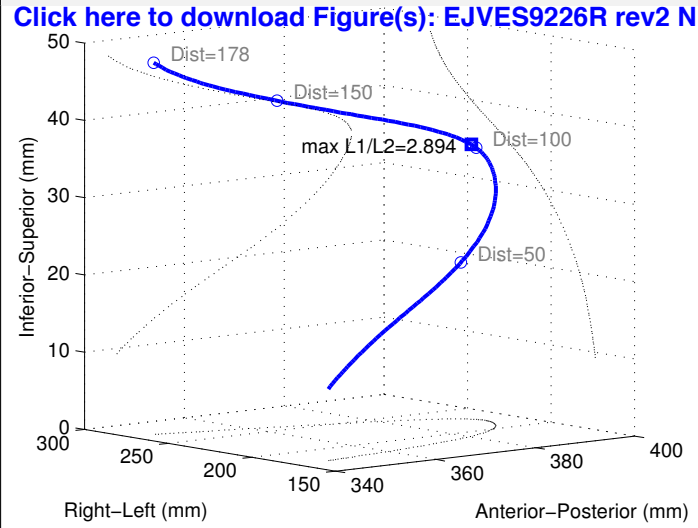

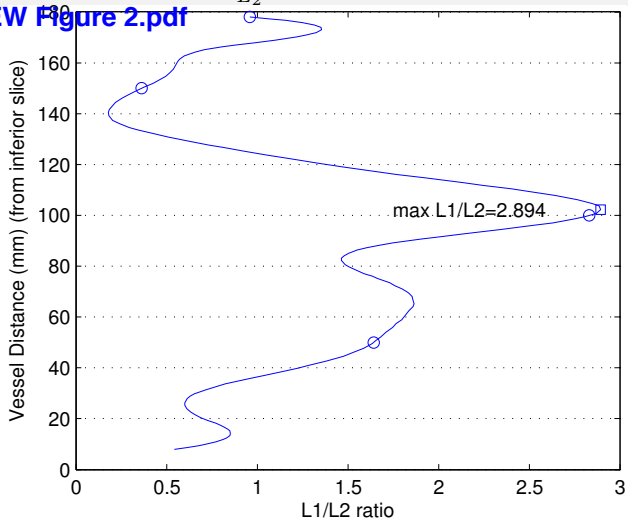

Example of *high* tortuosity medial line (using $\frac{L_1}{L_2}$-ratio)

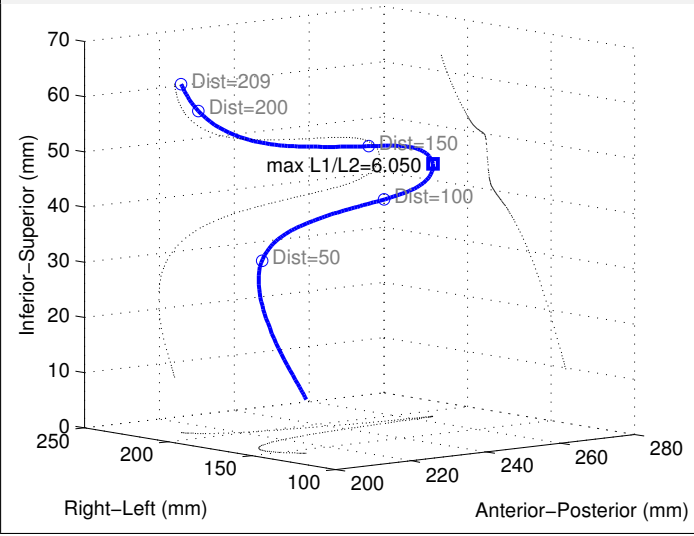

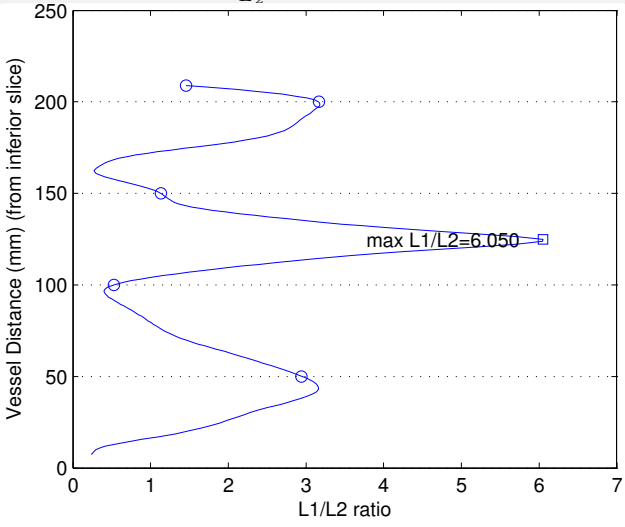

Figure(s) Ability to predict *early* problems using least tortuous artery at various scales

(a) ROC analysis of curvature

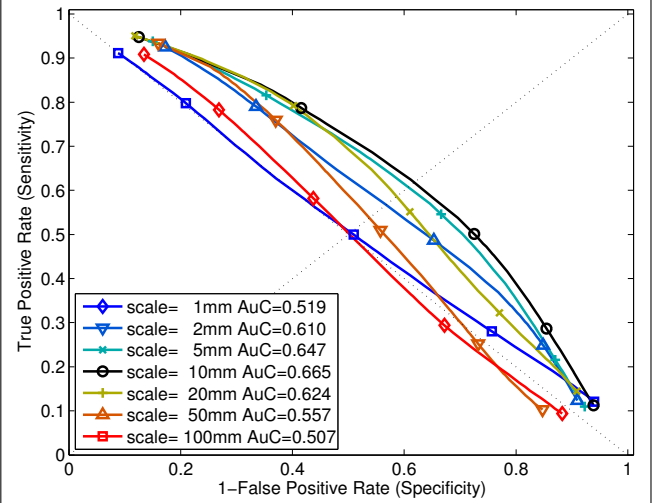

(b) Student t-test of curvature

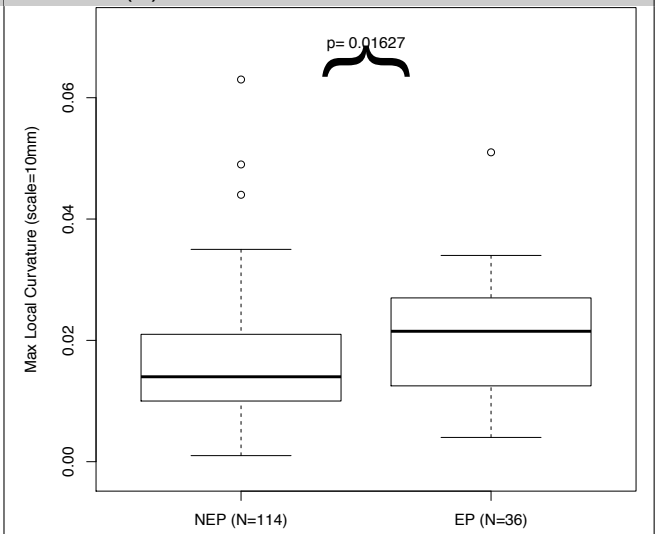

(c) ROC analysis of $\frac{L_1}{L_2}$ ratio

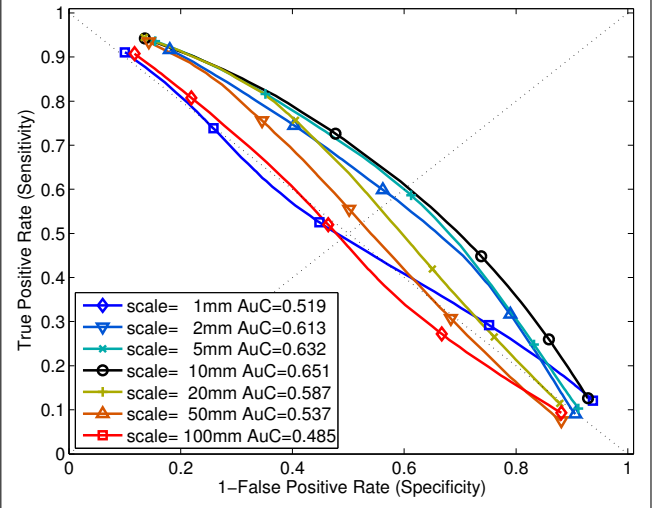

(d) Student t-test of $\frac{L_1}{L_2}$ ratio

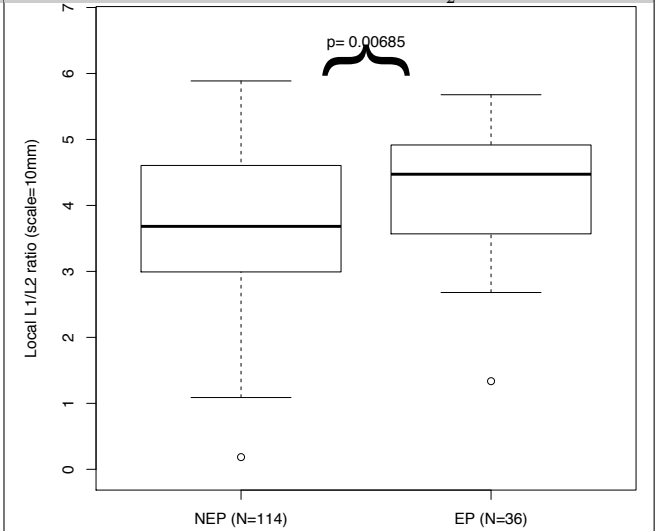

Figure(s) Ability to predict *late* problems using least tortuous artery at various scales

(a) ROC analysis of curvature (b) ROC analysis of $\frac{L_1}{L_2}$ ratio

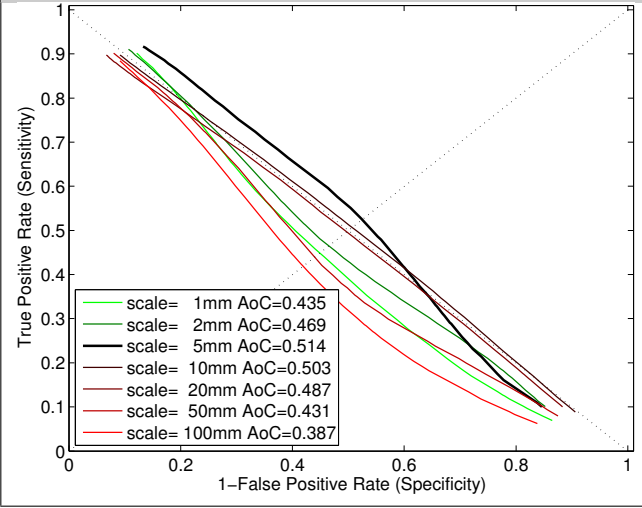

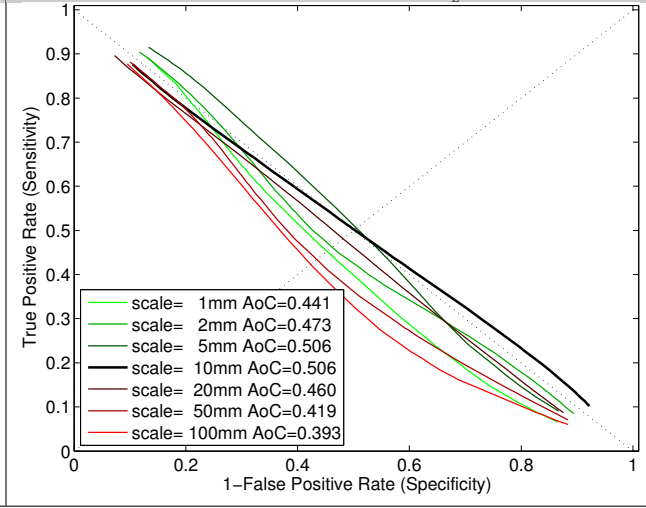

Figure(s) Ability to predict early problems of Maximum Aneurysm Diameter

(a) ROC analysis (b) Student t-test

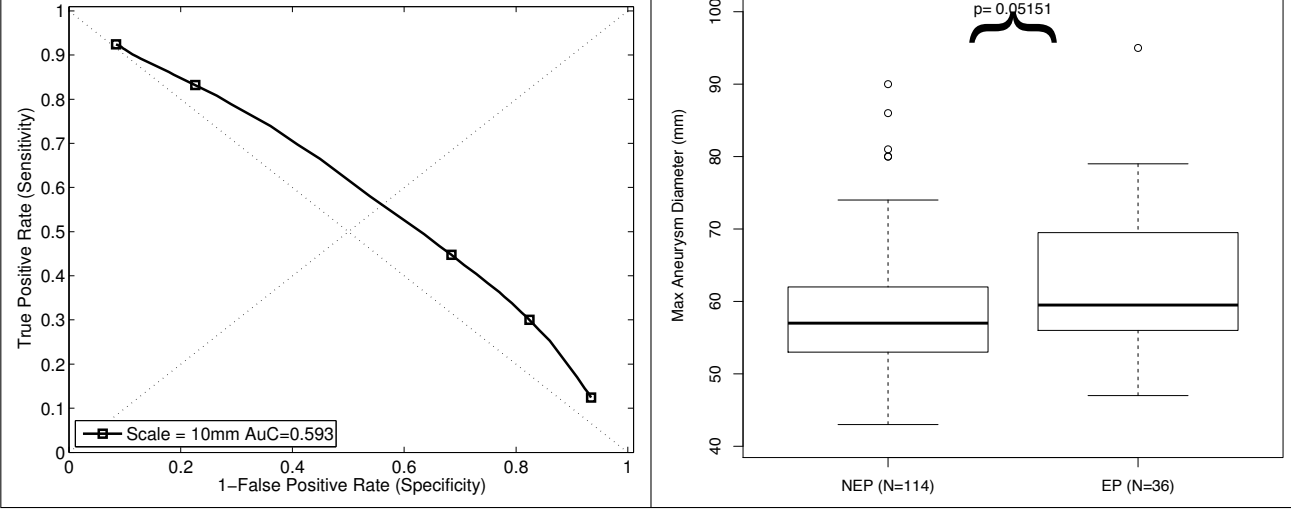

Figure(s)

Click here to download Figure(s): EJVES9226R rev2 Revised Figure 6.pdf

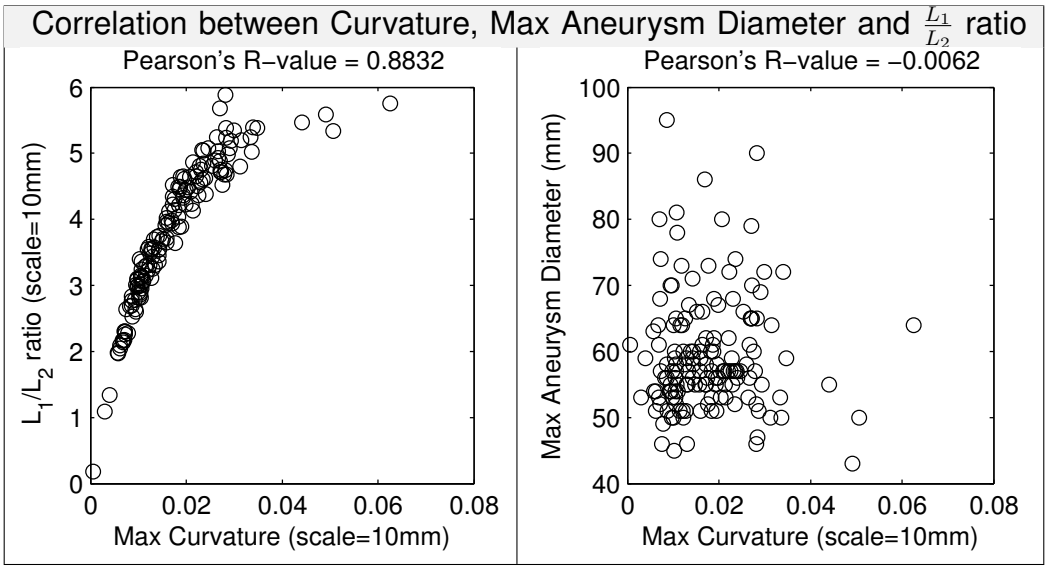

Supplementary Data online publication only

Click here to download Figure(s): EJVES9226R rev1 Supplementary Figure.pdf

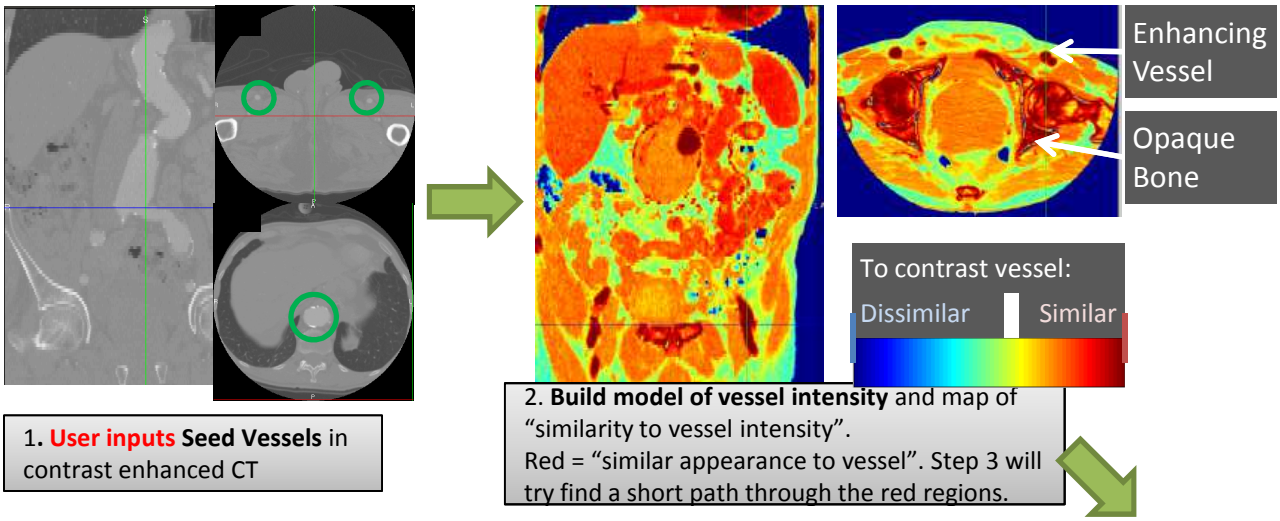

1. **User inputs Seed Vessels** in contrast enhanced CT

2. **Build model of vessel intensity** and map of "similarity to vessel intensity". Red = "similar appearance to vessel". Step 3 will try find a short path through the red regions.

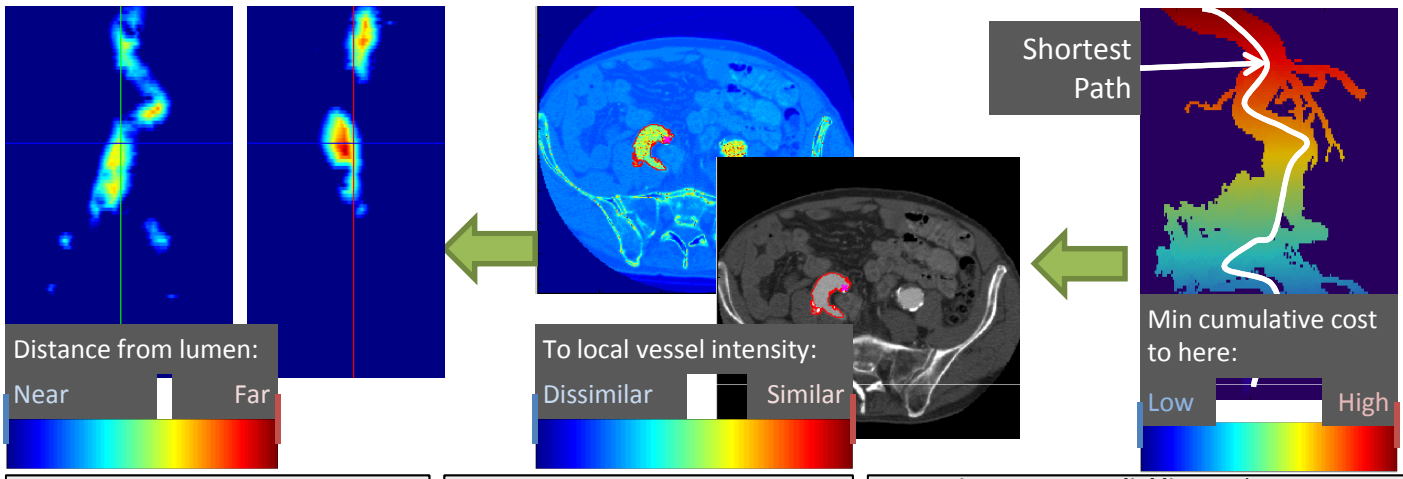

3. **Get inaccurate medial line**. Dijkstra algorithm to find short path. For this it explores all possible paths and builds a map of min cumulative cost to that point. Colours show internal cost map. **Output is the white line**.

4. **Refine Axial ROIs** to get better estimates of lumen using improved model of vessel intensity. Red = "similar to vessel"

5. **Measure distance from lumen with vessels.** Step 6 will try find a short path through the red regions

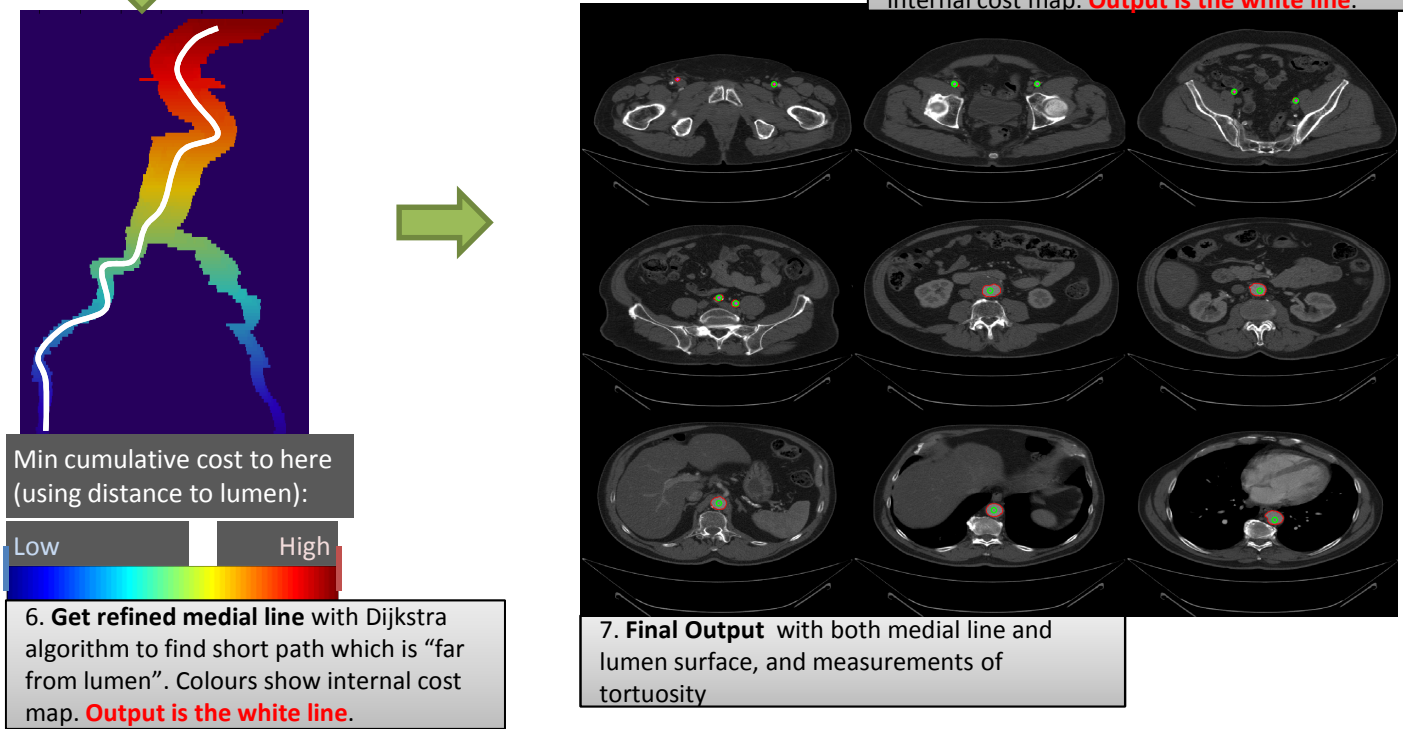

6. **Get refined medial line** with Dijkstra algorithm to find short path which is "far from lumen". Colours show internal cost map. **Output is the white line**.

7. **Final Output** with both medial line and lumen surface, and measurements of tortuosity

Supplementary Table

Click here to download Table(s): EJVES9226R_rev1_Supplementary_Table[1].doc

Early Problems (≤ 1 month)	Late Problems (> 1 month)	Peri-op Unplanned Procedures & Complications	1 month Post-op	6 months Post-op	1 year Post-op	2 years Post-op	3 years Post-op
Yes	Yes	Proximal neck extension. Type I Endoleak & kinking	Nil	No Data	Type I Endoleak	Nil	Nil
Yes	Yes	Stent extension. Type I & II Endoleak	Type I Endoleak	Type I Endoleak	Type I Endoleak	No Data	Nil
Yes	Yes	Misplaced deployment, IIA covered.	Nil	Nil	Nil	Kinking	
Yes	Yes	Nil	Thrombosis	Thrombosis	Thrombosis	Occlusion	Occlusion
Yes	Yes	Extension EIA/embolisation IIA	Nil	Migration	No Data	Nil	
Yes	Yes	Nil	Type I Endoleak	Type I Endoleak & Migration	Type I Endoleak	Nil	Nil
Yes	Yes	Type I Endoleak	Nil	Type I Endoleak	Nil	Deceased	
Yes	Yes	Nil	Stenosis	Kinking	Nil		
Yes	Yes	Nil	Stenosis	Stenosis	Nil		
Yes	Yes	Failed deployment - limb deployed in sac	Nil	No Data	Nil	Thrombosis	Deceased
Yes	Yes	Nil	Limb thrombosis	Kinking, limb thrombosis & Stenosis	Nil		
Yes	Yes	Type III Endoleak	Type III Endoleak	Endoleak & thrombosis	Deceased		
Yes	No	Nil	Kinking & occlusion	Deceased			

Yes	No	Nil	Deceased (myocardial infarct)				
Yes	No	Covered IIA	Nil	Nil	Nil	Nil	Nil
Yes	No	Type I Endoleak	Kinking & Stenosis	Nil	Nil	Nil	Nil
Yes	No	Proximal neck stent, extension to EIA/embolisation IIA.	Nil	Nil	Nil		
Yes	No	Type I Endoleak	Nil	No Data	Nil	Nil	Nil
Yes	No	Re-ballooning for Type I Endoleak	Nil	Deceased			
Yes	No	Covered renal artery	No Data	Nil	Nil	Nil	
Yes	No	EIA Angioplasty	Nil	Nil	Nil	Nil	
Yes	No	Stent to body/distal end graft.	Nil	Nil	Nil	Nil	
Yes	No	Nil	Thrombosis	Nil	Nil	Nil	
Yes	No	Misplaced deployment - IIA coil migration into EIA	Nil	Nil	Nil	Nil	Nil
Yes	No	Proximal neck extension.	Nil	Nil	Nil	Nil	
Yes	No	Stent to body/distal end graft	Nil	Nil	Nil	Nil	
Yes	No	Covered IIA	Nil	Nil	Nil	Nil	
Yes	No	Graft migration - covered renal artery	Nil	Nil	Nil	Deceased	

Yes	No	Proximal neck stent/extension. Type I Endoleak	Nil	No Data	Nil		
Yes	No	Misplaced deployment - top cap failed to disengage. Type I Endoleak	No Data	Nil	Nil		
Yes	No	Misplaced deployment - limb into EIA	Nil	Nil	Nil		
Yes	No	Stent to body/distal end graft	Nil	No Data			
Yes	No	Covered stent CIA, thrombectomy, ruptured iliac, limb occlusion & embolisation.	Deceased (TIA, renal failure, bradycardia, necrosis, MRSA)				
Yes	No	Type III Endoleak	Nil	Nil	Nil	No Data	Nil
Yes	No	Nil	Type III Endoleak				
Yes	No	Endarterectomy	Deceased (respiratory failure)				
No	Yes	Nil	Nil	Stenosis			
No	Yes	Nil	Nil	Nil	Kinking	Kinking	Kinking & Thrombosis
No	Yes	Nil	Nil	Nil	Kinking & occlusion	Nil	Nil

No	Yes	Nil	Nil	Nil	Kinking & stenosis	Kinking & stenosis	Stenosis
No	Yes	Nil	Nil	No Data	Thrombosis	Withdrawn	Withdrawn
No	Yes	Nil	Nil	Endoleak type unknown & stenosis	Type I Endoleak	Nil	
No	Yes	Nil	Nil	Stenosis	No Data	Stenosis	Nil
No	Yes	Nil	No Data	Nil	Nil	Nil	Type I Endoleak & Migration
No	Yes	Nil	Nil	Occlusion	Occlusion	No Data	Occlusion
No	Yes	Nil	Nil	Nil	Kinking	Occlusion	Occlusion
No	Yes	Nil	Nil	Type I Endoleak	No Data	Nil	
No	Yes	Nil	Nil	Nil	Type I Endoleak	Type I endoleak & migration - Sx open repair. Deceased - ruptured aneurysm	
No	Yes	Nil	Nil	Stenosis	Thrombosis & stenosis	Stenosis	
No	Yes	Nil	Nil	Nil	Nil	Migration	
No	Yes	Nil	Nil	Stenosis	Nil	No Data	Nil
No	Yes	Nil	Nil	Nil	Kinking & Stenosis	Nil	
No	Yes	Nil	Nil	Thrombosis	Nil	Nil	Nil
No	Yes	Nil	Nil	Thrombosis			
No	Yes	Nil	Nil	Thrombosis			

Supplementary Data online publication only

Click here to download Supplementary Data online publication only: EJVES9226R rev2 Supplementary Figure and Table Leg